Decreased Accessibility and Lack of Activation of ErbB2 in JIMT-1, a Herceptin-Resistant, MUC4-Expressing Breast Cancer Cell Line

Peter Nagy,[1] Elza Friedländer,[1,2] Minna Tanner,[3] Anita I. Kapanen,[3] Kermit L. Carraway,[4] Jorma Isola,[3] and Thomas M. Jovin[1]

[1]Department of Molecular Biology, Max Planck Institute for Biophysical Chemistry, Göttingen, Germany; [2]Department of Biophysics and Cell Biology, Medical and Health Science Center, University of Debrecen, Debrecen, Hungary; [3]Laboratory of Cancer Biology, Institute of Medical Technology, Tampere University and Tampere University Hospital, Tampere, Finland; and [4]Department of Cell Biology and Anatomy, University of Miami, School of Medicine, Miami, Florida

Abstract

Overexpression of erbB2 in breast tumors is associated with poor prognosis and is a target of receptor-oriented cancer therapy. Trastuzumab (Herceptin), a monoclonal antibody against a membrane-proximal epitope in the extracellular region of erbB2, shows a therapeutic effect against a fraction of *erbB2*-amplified breast tumors. Unfortunately, resistance to Herceptin is common, and its cause is as yet unclear. Here we investigated the properties of erbB2 in a Herceptin-resistant cell line, JIMT-1, established from a breast cancer patient showing *erbB2* gene amplification and primary resistance to Herceptin. The expression profile of erbB proteins, Herceptin-induced erbB2 internalization, and down-regulation in JIMT-1 were similar to those in Herceptin-sensitive lines. However, the mean number of Herceptin Mab binding sites in JIMT-1 was 1/5 that of the expressed erbB2 molecules, although 5% to 10% of the cells showed a ~10-fold higher Herceptin binding than the main population. Herceptin Fab and Mab 2C4, an antibody binding to an epitope in the ectodomain further removed from the membrane, bound more efficiently to JIMT-1 cells than Herceptin Mab, implying that erbB2 was partly masked. The expression of MUC4, a membrane-associated mucin that according to reports contributes to the masking of membrane proteins, was higher in JIMT-1 than in Herceptin-sensitive lines, and its level was inversely correlated with the Herceptin binding capacity of single cells. Knockdown of MUC4 expression by RNA interference increased the binding of Herceptin. Western blotting showed a low level of proteolytic processing, shedding, and tyrosine phosphorylation of erbB2 in JIMT-1. The latter finding may explain its Herceptin-resistant phenotype characterizing both the low and high Herceptin binding subpopulations. We conclude that masking of erbB2 in JIMT-1 leads to diminished Herceptin binding and isolation of erbB2 from its normal interaction and activation partners. (Cancer Res 2005; 65(2): 473-82)

Introduction

The erbB/HER family of transmembrane receptor tyrosine kinases consists of four proteins: erbB1 [epidermal growth factor (EGF) receptor, EGFR/HER1], erbB2/HER2, erbB3/HER3, and erbB4/HER4 (1). The limited signal transduction and transforming ability of single erbB proteins is significantly increased by extensive homoassociations and heteroassociations (2). The flexibility and scope of the network is further enhanced by the large number of activating peptide growth factors (3, 4). ErbB2 has no soluble high-affinity ligand (5) but fulfills a central role in the erbB signal transducing network by increasing the ligand binding spectrum (6) and affinity (7) of erbB1, erbB3, and erbB4. ErbB2 has a very potent intracellular tyrosine kinase domain conferring signaling superiority to its heterodimers by virtue of strong activation of both the mitogen-activated protein kinase and phosphatidylinositol 3-kinase (PI3K) pathways. The erbB2/erbB3 heterodimer is a very efficient "oncogenic unit" (8, 9). ErbB2-containing heterodimers are internalized less efficiently (10, 11) and evade lysosomal degradation (12), an effect which is even more pronounced upon erbB2 overexpression (13) also leading to ligand-independent constitutive activation of erbB2 homodimers (14, 15).

The overexpression of erbB2 observed in 20% to 30% of breast cancers identifies a patient group with poor prognosis (16). In addition to its prognostic value, erbB2 is the target of receptor-oriented cancer therapy (17), including trastuzumab (Herceptin), the first immunotherapeutic drug for the treatment of breast cancer (18, 19); 2C4, an antibody blocking heterodimerization of erbB2 (20); and CI-1033, a pan-erbB tyrosine kinase inhibitor (21).

Herceptin binds to a membrane proximal epitope in the extracellular region of erbB2 (22, 23). Its mode of action has been extensively studied, but the conclusive mechanism of action is still unknown. Herceptin induces internalization and down-regulation of erbB2. Although these phenomena are presumed to contribute to the therapeutic action (24), reports demonstrating the lack of correlation between the rate of internalization and the antibody's antiproliferative effect cast doubt on this model (25, 26). ErbB2 undergoes proteolytic cleavage by a metalloprotease, generating a soluble extracellular domain and a kinase active, tyrosine-phosphorylated 95-kDa intracellular fragment. This process is inhibited by Herceptin (27). Additionally, Herceptin treatment down-regulates phosphorylated Akt and increases the nuclear concentration of the cyclin-dependent kinase inhibitor p27KIP (28). Herceptin is a partial agonist of erbB2, an effect that requires further investigation (24, 29). Recently, genes have been identified that are either up-regulated or down-regulated during Herceptin treatment (30). In addition to these direct effects, antibody-dependent cellular cytotoxic reaction against Herceptin-targeted cells mediated by Fc receptors has also been invoked (31).

Although Herceptin constitutes a breakthrough in the treatment of advanced breast cancer, 70% of erbB2-overexpressing breast

Note: P. Nagy is currently at the Department of Biophysics and Cell Biology, Medical and Health Science Center, University of Debrecen, Nagyerdei krt. 98, Debrecen, H-4012, Hungary (E-mail: nagyp@jaguar.unideb.hu).

Requests for reprints: Thomas M. Jovin, Department of Molecular Biology, Max Planck Institute for Biophysical Chemistry, Am Fassberg 11, Göttingen, Germany 37077. Phone: 49-551-2011381; Fax: 49-551-2011467; E-mail: tjovin@gwdg.de.

Table 1. Expression levels of erbB proteins and Herceptin-induced internalization and down-regulation of erbB2

	JIMT-1	SKBR-3	BT-474	MDA-453
Expression level ($\times 10^3$)				
erbB1	160	190	16	60
erbB2	620	1,100	1,450	620
erbB3	10	42	20	18
erbB4	0	0	0	2
IGF-1R	5	4	9	5
Herceptin internalization (%)	33 ± 4	25 ± 1	22 ± 2	16 ± 2
Herceptin-induced erbB2 down-regulation (%)	40 ± 5	31 ± 2	27 ± 2	38 ± 3

NOTE: The expression levels of proteins were determined by flow cytometry. The following antibodies were used: Ab1-Clone 528 (erbB1), Ab3/OP15 (erbB2), Ab4-Clone H3.90.6 (erbB3), Ab1-Clone H4.77.16 (erbB4), and Ab1-Clone 24-31 (IGF1R). For the determination of Herceptin-induced effects, cells were treated with 10 μg/mL Herceptin. Herceptin internalization and Herceptin-induced erbB2 down-regulation were determined at 3 and 48 hours of Herceptin treatment, respectively. Herceptin internalization is expressed as the percentage of the initial level of bound Herceptin. ErbB2 down-regulation values represent the percentage by which erbB2 expression was reduced after 48 hours of Herceptin treatment, compared with untreated samples.

cancers show primary resistance to Herceptin as a single agent (32). Although the response rate to Herceptin when combined with chemotherapy is somewhat higher (33), continued administration of the antibody inevitably leads to secondary resistance.

The molecular mechanisms accounting for Herceptin resistance in patients are currently unknown. Autocrine production of EGF-like ligands (34), overexpression of insulin-like growth factor 1 receptor (IGF-1R; ref. 35) and production of an alternatively spliced, intracellularly retained extracellular domain of erbB2 (36) have been invoked as possible causes. The common denominator is the presence of an erbB2-independent means for the constitutive activation of the PI3K pathway.

Blocking of Herceptin binding by MUC4, a cell surface mucin, has also been implicated in Herceptin resistance. It has been shown that overexpression of rat Muc4 reduces binding of Herceptin to erbB2-expressing tumor cells (37). However, it remains unclear whether human MUC4 fulfills a similar role. MUC4 is a membrane-associated, highly glycosylated mucin consisting of two parts: MUC4β, a 90-kDa transmembrane subunit containing EGF-like domains and MUC4α, a noncovalently associated, heavily *O*-glycosylated soluble mucin subunit (38). The latter contains a large tandem repeat domain varying in length between 3285 and 7285 amino acids (39, 40). Consequently, the molecular weight of the soluble subunit varies between 500 and 900 kDa, and the whole molecule extends ~1 to 2 μm from the cell surface. Mucins provide a protective coat to epithelia (38). Cancers often overexpress MUC4 and usurp its protective function to inhibit cellular and antibody-mediated immune attack (37, 41) or to increase their metastatic potential (42). Inhibition of MUC4 expression suppresses the growth and metastatic potential of pancreatic cancer cells (43). Furthermore, Muc4 of rat origin is reported to be a membrane-associated ligand of erbB2 (44, 45).

In the current paper, we examine the mechanisms of Herceptin resistance in JIMT-1 cells, a line recently established from a Herceptin-resistant breast cancer patient. It has been shown that JIMT-1 retained erbB2 amplification and overexpression as well as Herceptin resistance as a stable phenotype.[5] We show that the Herceptin binding epitope of erbB2 in JIMT-1 was masked, probably by MUC4, leading to diminished binding of Herceptin. RNA interference (RNAi)–mediated suppression of MUC4 expression increased Herceptin binding to the cells. Both shedding and tyrosine phosphorylation of erbB2 were low in JIMT-1 cells, presumably due to sequestration of erbB2 away from its natural interaction partners. Although a minor subpopulation of JIMT-1 showed ~10 times higher Herceptin binding than the main subpopulation, both were Herceptin resistant.

Materials and Methods

Cells. SKBR-3, BT-474, and MDA-453 cell lines were obtained from the American Type Culture Collection (Rockville, MD) and cultured according to their specifications. The JIMT-1 breast cancer line isolated from the pleural effusion of a Herceptin-resistant breast cancer patient was grown in F12/DMEM (1:1) supplemented with 10% FCS, 60 units/L insulin and antibiotics.[5] For flow cytometric experiments, cells were harvested with a PBS-based enzyme-free cell dissociation buffer (Invitrogen, Carlsbad, CA).

Antibodies, Growth Factors, and Chemicals. Staining of cell surface erbB1, erbB3, erbB4, and IGF-1R was carried out with Ab1-Clone 528, Ab4-Clone H3.90.6, Ab1-Clone H4.77.16, and Ab1-Clone 24-31 (all from LabVision, Fremont, CA), respectively, followed by fluorescent secondary antibody. Labeling of erbB2 was either carried out with the Ab3/OP15 antibody (Calbiochem-Merck Biosciences, Schwalbach, Germany) on fixed (3.7% HCHO, 30 minutes) and permeabilized (0.1% Triton X-100) cells followed by secondary labeling or with fluorescent 2C4 antibody, Herceptin antibody or Fab (all from Genentech, South San Francisco, CA) on nonpermeabilized cells. Labeling of primary antibodies or Fabs with Alexa dyes was carried out according to the manufacturer's specifications (Molecular Probes, Eugene, OR). Calibration of fluorescent signals in terms of number of binding sites per cell was done with Qifikit (DakoCytomation, Glostrup, Denmark). The 1G8 antibody against the membrane-associated β subunit of MUC4 was developed in one of our laboratories (KLC). It has been shown that 1G8 recognizes a band corresponding to the expected molecular weight of human MUC4β in Western blotting, and it specifically stained cells expressing human MUC4 in immunofluorescence experiments (46). 1G8

[5] Rennstam et al., submitted for publication.

was applied to fixed and Triton X-100–treated cells followed by secondary labeling with Cy2-goat anti-mouse Fab (Jackson Immunoresearch, West Grove, PA). All steps of primary and secondary labelings were carried out on ice. Heregulin-β1 was purchased from R&D Systems (Minneapolis, MN), and was used at a concentration of 100 ng/mL. Aminophenylmercuric-acetate (APMA) was from Sigma (Schnelldorf, Germany).

Flow and Image Cytometry. A Coulter Epics Elite flow cytometer was used to quantitate expression levels of proteins labeled by fluorescent antibodies. Analysis of flow cytometry data was carried out with FCS Express V2 (De Novo Software, Thornhill, Ontario, Canada). Optical sections of cells were acquired with a Zeiss LSM510 confocal laser scanning microscope. General image analysis (smoothing, registration) and quantitation of fluorescence intensities were done with Scil-Image (University of Amsterdam, The Netherlands). Pixel-by-pixel analysis of colocalization between MUC4 and Herceptin was done with a program written in LabView 5.1 (National Instruments, Austin, TX).

Calculation of the Relative Number of Antibody Binding Sites on Different Cell Lines. Cells were labeled with OP15, Herceptin Mab (in the presence or absence of Triton X-100), Herceptin Fab, 2C4 Mab as described above, and fluorescence intensities were determined using flow cytometry. The mean fluorescence intensities of JIMT-1 and BT-474 cells were divided by the corresponding mean intensities of SKBR-3. The resultant ratio was divided by the erbB2 expression ratio for the given cell pair (JIMT-1/SKBR-3 = 0.56; BT-474/SKBR-3 = 1.32; determined by Qifikit), so that the normalized ratio reflected whether the given epitope was equally exposed on the two cell lines (i.e., a value of 1 corresponded to equal exposure).

Internalization of Herceptin. Cells in suspension were incubated with 10 μg/mL Alexa633-labeled Herceptin at 37°C for 0 to 3 hours. Subsequently, 1/2 of the samples were treated with a 15-fold excess of acid strip buffer [0.5 mol/L NaCl, 0.1 mol/L glycine (pH 2.8)] for 3 minutes on ice followed by washing and resuspension in PBS. Cells were analyzed by flow cytometry, and the internalized fraction of Herceptin was calculated by dividing the mean fluorescence intensity of the acid stripped sample with that of the untreated control.

Western Blotting. Whole cell lysates were prepared in 2× SDS sample buffer [125 mmol/L Tris-HCl (pH 6.8), 4% SDS, 20% glycerol, 100 mmol/L DTT, 0.02% bromphenolblue] or in lysis buffer [20 mmol/L Tris-HCl (pH 7.5), 150 mmol/L NaCl, 10% glycerol, 1 mmol/L EGTA, 1 % Triton X-100, 1 Complete Mini (Roche, Mannheim, Germany) protease inhibitor cocktail tablet/10 mL, 1 mmol/L Na_3VO_4, 1 mmol/L phenylmethylsulfonyl fluoride, 10 mmol/L NaF, 10 mmol/L β-glycerol phosphate, 10 mmol/L $Na_4P_2O_7$]. Immunoprecipitation of erbB2 was carried out with Herceptin or Ab3-OP15 for 1 hour on ice and Sepharose 4B Fast Flow Protein G beads (Sigma). Immunoprecipitates or whole cell lysates were resolved on 4% to 12% Novex Bis-Tris SDS-polyacrylamide gradient gels (Invitrogen) and blotted to nitrocellulose membranes. The following antibodies were used for primary labeling of the membranes at dilutions suggested by the manufacturers: Ab3-OP15 and Ab20 (L87 + 2ERB19; LabVision) for the intracellular and extracellular parts of erbB2, respectively; Ab18-PN2A (LabVision) for erbB2 phosphorylated at Y1248, PY99-sc7020 (Santa Cruz Biotechnology, Santa Cruz, CA) for phosphotyrosine; and 1G8 for MUC4 and A4700 (Sigma) for actin. Peroxidase-conjugated goat anti-mouse IgG and an enhanced chemiluminescence kit (Amersham, Freiburg, Germany) were used for detection.

Detection of ErbB2 Ectodomain Shedding by ELISA. The shed ectodomain of erbB2 was analyzed from undiluted cell culture media using a commercially available enzyme immunoassay kit (Bender MedSystems, Vienna, Austria) according to the manufacturer's instructions. The detection threshold for soluble erbB2 was 0.1 ng/mL.

Reverse Transcription-PCR of MUC4 mRNA. Reverse transcription-PCR was used to study *MUC4* gene expression in JIMT-1 and control cells lines (SKBR-3 and BT-474). Lung tissue was used as a known positive control. Total RNA was extracted using GenElute Mammalian Total RNA kit (Sigma Chemical Co., St. Louis, MO). Reverse transcription of *MUC4* and glyceraldehyde-3-phosphate dehydrogenase (*GAPDH*) reference gene was done using 2.5 μg of total RNA as a template according to the manufacturer's instructions (Supercript First-Strand Synthesis System for reverse transcription-PCR, Invitrogen). The first strand cDNA synthesis product (1/10 volume) was used as a starting material in subsequent PCR amplification. PCR for *MUC4* was done as follows: initial denaturation (95°C for 4 minutes), denaturation (94°C for 1 minute), annealing (58°C for 1 minute), and extension (72°C for 1 minute), 30 cycles. PCR for *GAPDH*: denaturation (94°C for 30 seconds), annealing (62°C for 45 seconds), and extension (72°C for 45 seconds), 30 cycles. The primers for *MUC4* were 5′-CTGGATGGTCATCTCGGAGT-3′ and 5′-TCGAGTTTCATGCTCAGGTG-3′ and for *GAPDH* were 5′-TCCTGGAAGATGGTGATGGGAT-3′and 5′-TGAAGGTCGGAGTCAACGGATT-3′. *MUC4* expression levels were evaluated relative to *GAPDH*.

RNAi. Twenty-one–nucleotide double-stranded small interfering RNA (siRNA) with two-nucleotide 3′ overhangs (antisense strand GUGAAGUCCGAUGCUUGCGTT and sense strand CGCAAGCAUCGGACUUCACTT) against human MUC4 was synthesized by Qiagen (Hilden, Germany). The above sequence is present in all splice variants of MUC4 characterized thus far. A control siRNA against green fluorescent protein (ref. 47; antisense strand GUUCACCUUGAUGCC GUUCTT and sense strand GAACGGCAUCAAGGUGAACTT) was synthesized by T. Tuschl (currently at Rockefeller University, New York, NY). A BLAST analysis revealed no known unintended targets of the above siRNAs. Transfection of JIMT-1 cells with 100 nmol/L siRNA was carried out with Oligofectamine (Invitrogen) according to the manufacturer's specifications and protein expression and the phenotype of cells were analyzed 48 hours after transfection.

Results

The Expression of ErbB Family Members and Herceptin-Induced ErbB2 Internalization and Down-Regulation Are Not Significantly Different in JIMT-1 Cells from Herceptin-Sensitive Lines. Altered expression of erbB proteins is thought to be causally related to the malignant phenotype. Therefore, we investigated whether the expression levels of erbBs in the Herceptin-resistant JIMT-1 line were different from those in three Herceptin-sensitive lines, SKBR-3, BT-474 and MDA-453. Although the differences between the cell lines were substantial (Table 1), they probably cannot account for the Herceptin resistance of JIMT-1 because the expression levels of erbB proteins in JIMT-1 were in the same range as in the other cell lines. In particular, the expression profile of MDA-453 was very similar to that of JIMT-1 (Table 1). IGF-1R, the overexpression of which has been suggested to induce Herceptin resistance, was present in JIMT-1 at approximately the same level as in the other cell lines. We also measured the internalization of Herceptin and down-regulation of erbB2 induced by Herceptin (Table 1). Both of these processes took place as efficiently in JIMT-1 as in the Herceptin-sensitive cell lines. We conclude that impaired Herceptin internalization or erbB2 down-regulation does not account for the Herceptin resistance of JIMT-1.

The Epitope of Herceptin Was Masked in JIMT-1 Cells. Inasmuch as the number of erbB2 molecules in JIMT-1 cells was determined with an antibody specific for an intracellular epitope, it was still possible that Herceptin binding was impaired. Indeed, although the expression of erbB2 in JIMT-1 was ~50% that of SKBR-3 cells, the relative Herceptin binding capacity of JIMT-1 was ~10% that measured in SKBR-3, implying that only 1 of 5 erbB2 proteins constitute a Herceptin binding site in JIMT-1 cells (Fig. 1*A*). The diminished binding of Herceptin to JIMT-1 cells was

unique to this line, because it was not observed in BT-474. We also determined the dissociation constant for Herceptin binding to erbB2 on the three breast cancer cell lines. These measurements also showed that Herceptin binding to JIMT-1 was compromised, but the dissociation constants were not strongly correlated with the Herceptin-resistant phenotype [JIMT-1, 1.5 μg/mL (10 nmol/L); SKBR-3, 0.6 μg/mL (4 nmol/L); BT-474, 1 μg/mL (6 nmol/L)]. Next, we tested whether the binding of Herceptin to JIMT-1 could be increased by fixing and permeabilizing the cells before labeling. Triton X-100–permeabilized JIMT-1 cells showed a remarkably higher Herceptin binding capacity than their unpermeabilized counterparts, whereas the binding of Herceptin to SKBR-3 or BT-474 cells was not substantially affected (Fig. 1*A* and *B*). Furthermore, JIMT-1 cells showed a binding capacity for both Herceptin Fab and 2C4 Mab exceeding that of Herceptin Mab. Labeling with Herceptin Fab and 2C4 Mab was done on nonpermeabilized cells, excluding that increased Herceptin Mab binding to JIMT-1 after permeabilization cells was caused by the sequestration of erbB2 in an intracellular pool. Sequencing of the entire coding sequence of erbB2 in JIMT-1 revealed no mutations,[6] from which we tentatively conclude that masking of the Herceptin epitope in JIMT-1 accounted for the diminished binding of the antibody.

The Local Density of the Membrane-Associated Mucin, MUC4, Was Negatively Correlated with Herceptin Binding. It had been reported previously that overexpression of rat Muc4 results in reduced binding of antibodies against the extracellular region of erbB2 (37). Fluorescence microscopy (Fig. 1*B*), Western blotting (Fig. 2*A*), and reverse transcription-PCR (Fig. 2*B*) showed that MUC4 was expressed at a substantially higher level in JIMT-1 than in the Herceptin-sensitive breast tumor cell lines. On Western blots, the anti MUC4 Mab 1G8 recognized a ~120-kDa protein, corresponding to the approximate molecular weight of the membrane-bound subunit of MUC4. JIMT-1 cells labeled with 1G8 and Herceptin showed an inverse correlation between the local density of MUC4 and Herceptin binding (Fig. 2*C*). A two-dimensional histogram of Herceptin and 1G8 fluorescence intensities revealed that the negative correlation manifested itself primarily in the high intensity pixels, which displayed either high MUC4 density or high Herceptin binding but not both, implying that high MUC4 expression interfered with the binding of Herceptin (Fig. 2*D*).

RNAi–Mediated Suppression of MUC4 Expression Increased Herceptin Binding. RNAi is a highly efficient means for the selective suppression of gene expression (48). We designed a siRNA against human MUC4 that is homologous to all known splice variants of the protein. The MUC4 siRNA proved to be an efficient suppressor of MUC4 expression when transfected to JIMT-1 (Fig. 3*A*). Although the fraction of cells transfected with the siRNA was low (~15%), the suppression efficiency was ~100% in these cells, as reflected by the superposition of the peaks corresponding to the transfected cells and the unlabeled control. Specificity of the RNAi effect is supported by the absence of inhibition of MUC4 expression by a nonspecific siRNA (Fig. 3*A*) and by the lack of knockdown of actin expression by the MUC4 siRNA (Fig. 3*B*). Herceptin staining of

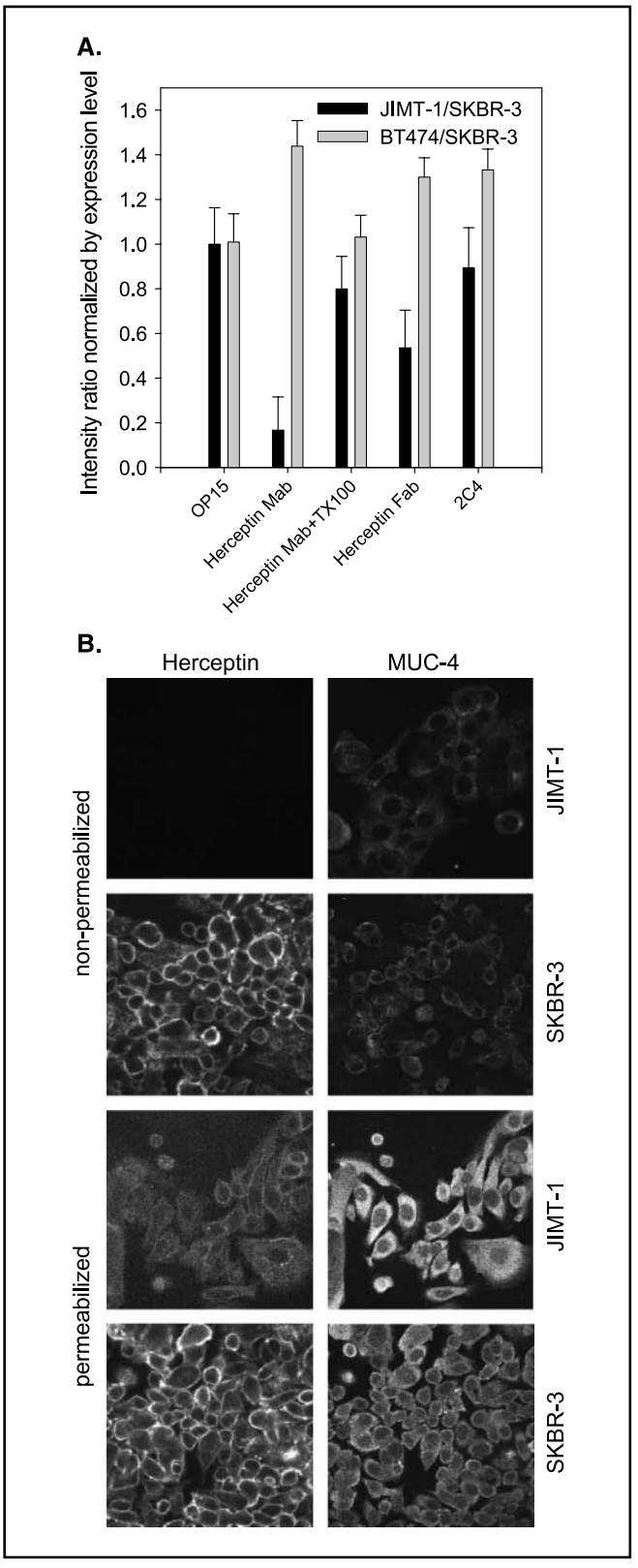

Figure 1. Masking of the Herceptin epitope on erbB2 in JIMT-1 cells. *A,* cells labeled with the indicated antibodies and analyzed by flow cytometry. Intensity ratios JIMT-1/SKBR-3 and BT-474/SKBR-3 were determined and normalized as described in MATERIALS AND METHODS. *Bars,* SE. *B,* cells cultured on glass coverslips and stained with Herceptin or 1G8 (against MUC4) with or without permeabilization with 0.1% Triton X-100. Imaging was with identical microscope settings.

[6] Tanner et al., unpublished observation.

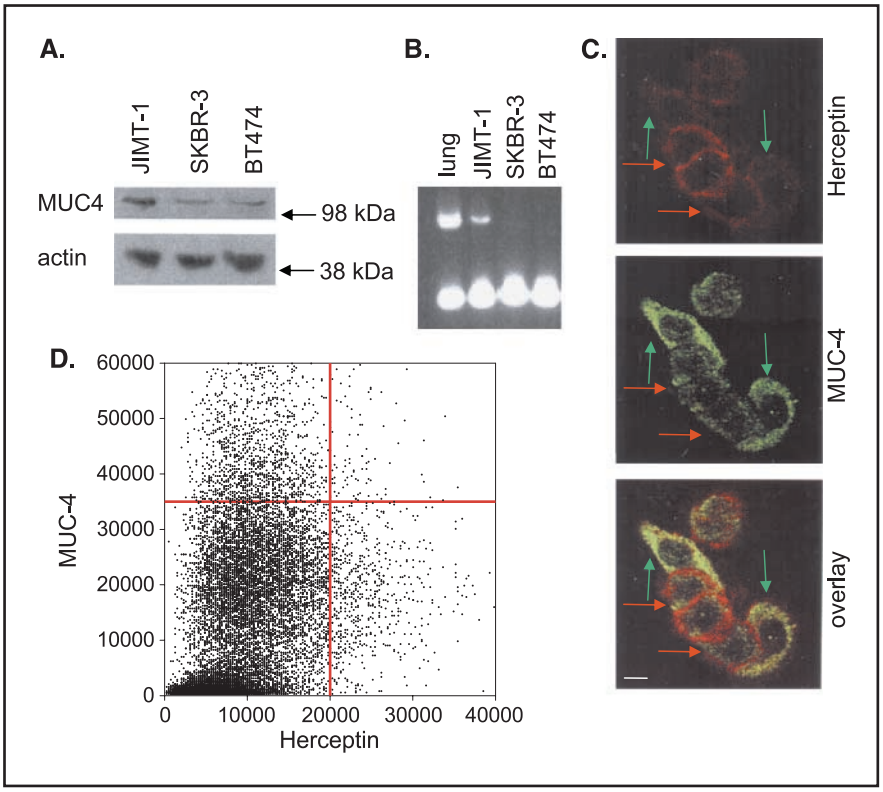

Figure 2. MUC4 was highly expressed in JIMT-1 cells and its local density was negatively correlated with Herceptin binding. *A,* whole cell lysates separated by SDS-PAGE, and blotted with 1G8 antibody against MUC4. Membranes were stripped and reprobed with A4700 antibody against actin. *B,* reverse transcription-PCR amplification of MUC4 (*top bands*, 414 bp) and GAPDH (*bottom bands*, 204 bp). *C,* JIMT-1 cells grown on coverslips, fixed in 3.7% HCHO and permeabilized with 0.1% Triton X-100. Cells were labeled with Cy5-Herceptin (*red channel*) and with 1G8 against MUC4 followed by secondary labeling with Cy2-goat anti-mouse Fab (*green channel*). *Green arrows,* regions with high MUC4 and low Herceptin intensity; *red arrows,* low MUC4 and high Herceptin regions. Bar, 10 μm. *D,* two-dimensional histogram of 1G8 intensity versus Herceptin intensity. Cells double-labeled as in *C* were thresholded to yield a mask containing pixels with higher than background Herceptin intensity. The two-dimensional histogram was calculated for pixels in the Herceptin mask.

nonspecific siRNA-transfected or -untransfected JIMT-1 cells yielded a bimodal distribution; ~10% of the cells showed high Herceptin binding. The size of the subpopulation with bright Herceptin staining was higher in the MUC4 siRNA–transfected sample, and the increase (~15%) corresponded well with the fraction of cells with no MUC4 expression (Fig. 3*C*). We did fluorescence-activated cell sorting on Herceptin-stained cells and separated the two subpopulations. Western blotting of the sorted cells revealed that MUC4 expression was negatively correlated with the Herceptin binding capacity (Fig. 3*C*).

ErbB2 Was Less Tyrosine Phosphorylated in JIMT-1 Cells than in Herceptin-Sensitive Lines. Overexpressed erbB2 is phosphorylated on tyrosine residues (13). Although JIMT-1 overexpressed erbB2, we could detect only very low levels of tyrosine phosphorylation of erbB2 in whole cell lysates of normally cultured JIMT-1 cells using an antibody specific for erbB2 phosphorylated on

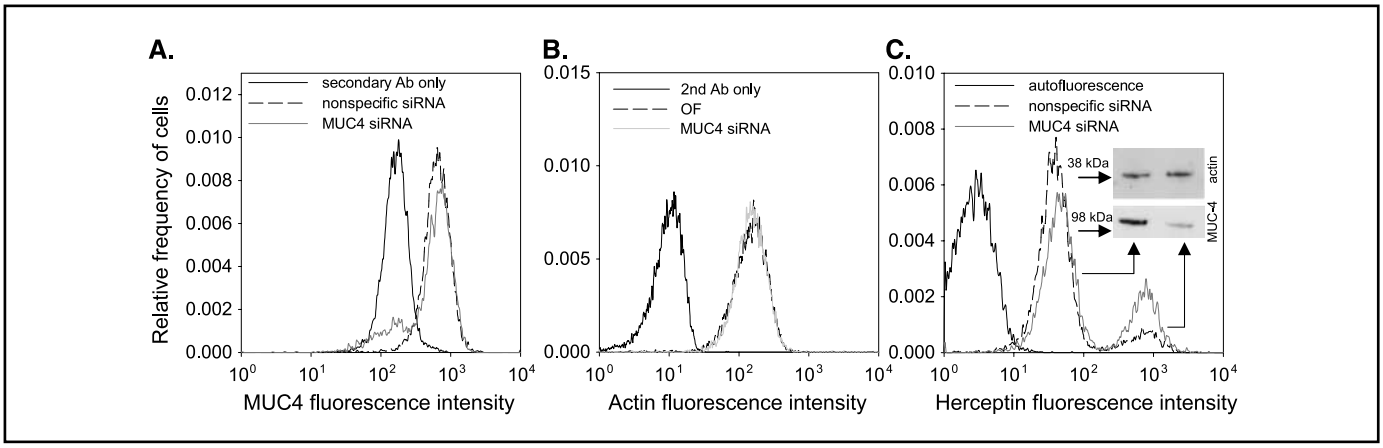

Figure 3. RNAi-mediated knockdown of MUC4 expression increased Herceptin binding. *A* and *B,* flow cytometry of JIMT-1 cells transfected with a nonspecific siRNA or a siRNA against MUC4. Cells were removed from the plates with enzyme-free cell dissociation buffer 48 hours after transfection or treatment with oligofectamine (*OF*) only, and MUC4 (*A*) or actin (*B*) expression was analyzed by flow cytometry. *C,* flow sorting and Western blotting of siRNA-transfected cells. Cells transfected with a nonspecific siRNA or MUC4 siRNA were stained with Cy5-Herceptin and analyzed by flow cytometry. An equal number (20,000) of cells in the subpopulations with high and low Herceptin binding were sorted, and their MUC4 and actin expressions were determined by Western blotting.

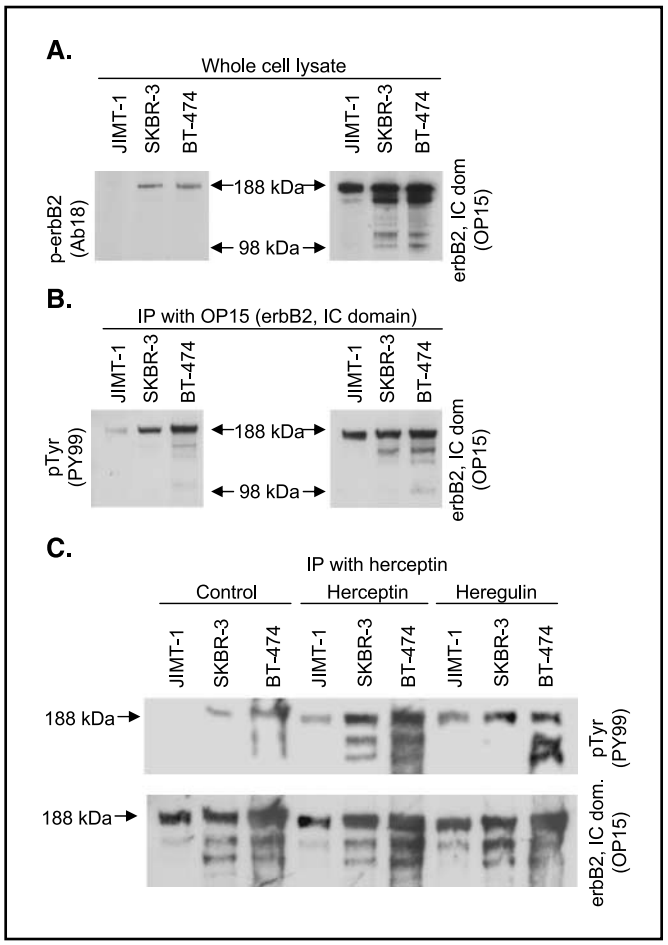

Figure 4. Low level of tyrosine phosphorylation of erbB2 in JIMT-1 cells. *A,* whole cell lysates of breast cancer cell lines. Lysates of cells kept under standard culture conditions were electrophoresed by SDS-PAGE and transferred to nitrocellulose. Membranes were blotted with an antibody against erbB2 phosphorylated on Tyr1248, then stripped and reprobed with OP15 (anti-erbB2 Mab) to show equal loading of full-length erbB2. *B,* ErbB2 immunoprecipitated with OP15 from whole cell lysates probed with an antiphosphotyrosine antibody followed by stripping and reprobing with OP15. Cells were kept under normal culture conditions. *C,* ErbB2 immunoprecipitated from lysates of cells exposed to Herceptin or heregulin, electrophoresed and probed with an antiphosphotyrosine Mab (PY99) and then stripped and reprobed with OP15. Cells were starved in the absence of serum for 24 hours. Control samples and cells treated with 10 μg/mL Herceptin or with 100 ng/mL heregulin for 10 minutes at 37°C were lysed, and erbB2 was immunoprecipitated with Herceptin, and was resolved by SDS-PAGE.

Tyr 1248 (Fig. 4*A*) or on Herceptin-immunoprecipitated erbB2 with a phosphotyrosine-specific Mab (Fig. 4*B*). Under the same experimental conditions, erbB2 was heavily tyrosine phosphorylated on SKBR-3 and BT-474. Reprobing the membranes with an anti-erbB2 antibody showed approximately equal loading of full-length erbB2. A 24-hour starvation in the absence of serum decreased but did not eliminate erbB2 tyrosine phosphorylation in SKRB-3 and BT-474 (Fig. 4*C*). Stimulation with Herceptin or heregulin led to elevated erbB2 tyrosine phosphorylation in all three breast cancer lines, but the increase in JIMT-1 was much smaller than in SKBR-3 or BT-474.

Shedding of ErbB2 Ectodomain Was Reduced in JIMT-1. Bands corresponding to proteolytic products, including the NH_2-terminally truncated $p95^{erbB2}$, were absent from or very weak on Western blots of JIMT-1 but were prominent on blots from SKBR-3 and BT-474 (Fig. 4). To establish that the lower molecular weight bands were NH_2-terminally truncated intracellular fragments of erbB2, we blotted whole cell lysates of the breast cancer cell lines with OP15, an antibody recognizing an intracellular epitope on erbB2, followed by stripping and reprobing with Ab20 against the extracellular region of erbB2 (Fig. 5*A*). The failure of Ab20 to recognize the low molecular weight bands in the SKBR-3 and BT-474 lanes proved that these were indeed NH_2-terminally truncated fragments. We confirmed these results with similar experiments done on immunoprecipitated erbB2 (Fig. 5*B*). In addition, despite the fact that bands corresponding to full length erbB2 on the OP15 blots showed comparable intensities in the case of all three breast cancer lines, the signal was very weak or absent in the JIMT-1 lane on the Ab20 blots (Fig. 5*A* and *B*), indicating that the epitope recognized by Ab20 was altered in JIMT-1. This finding needs further investigation.

ELISA detection of the shed erbB2 ectodomain showed a reduced level of soluble erbB2 in the conditioned medium of JIMT-1 compared with SKBR-3 or BT-474 (Fig. 5*C*). ErbB2 was shed from JIMT-1 to a lesser extent even taking into consideration the 2-fold lower expression level of erbB2 in JIMT-1.

Metalloprotease-Mediated Cleavage Unmasked the Herceptin Binding Site on ErbB2. APMA is an activator of metalloproteases. SKBR-3 and BT-474 cells were treated with 1 mmol/L APMA, and subsequently stained with fluorescent 2C4 to quantitate the amount of erbB2 on the cell surface. These experiments revealed that APMA decreased the cell surface expression of erbB2 in SKBR-3 and BT-474 by ~20% (Fig. 6*A*) in accordance with previous results (27). APMA treatment of JIMT-1 cells resulted in a ~40% increase in 2C4 binding. APMA induced a ~10-fold increase in Herceptin binding to SKBR-3 and BT-474 (Fig. 6*B* and *D*), and a ~40-fold increase in JIMT-1 (Fig. 6*B* and *C*). APMA-activated metalloproteases also cleaved membrane proteins other than erbB2 including those that mask it (e.g., MUC4). This may have lead to increased exposure of erbB2 epitopes, although the total number of membrane-bound erbB2 extracellular domains decreased. These findings corroborate that the Herceptin epitope was masked in JIMT-1 and to a lesser degree in Herceptin-sensitive lines as well. The enhanced 2C4 binding to APMA-treated JIMT-1 cells indicated that the membrane-distant 2C4 epitope was also masked to some extent.

Double labeling of untreated breast cancer cell lines with Mabs 2C4 and Herceptin showed that the two subpopulations of JIMT-1 cells showing different capacities for Herceptin binding (Figs. 3*C* and 6*C*) expressed erbB2 equally on the cell surface (Fig. 6*E*) providing further evidence for masking of the Herceptin epitope. The heterogeneity in SKBR-3 and BT-474 with respect to Herceptin binding capacity was negligible compared with that observed in JIMT-1 (Fig. 6*E* and *F*).

The Subpopulations Showing High and Low Herceptin Binding Capacity Are Equally Resistant to Herceptin. JIMT-1 cells were treated with 10 μg/mL Herceptin for 5 days with replenishment of Herceptin containing medium every 2nd day. Cell counting revealed that Herceptin did not slow the proliferation of JIMT-1 (2.9 ± 0.4- and 3.3 ± 0.4-fold increase in cell number in the absence and presence of Herceptin, respectively). The size of the high Herceptin binding subpopulation determined by flow cytometry in Herceptin-treated (8 ± 2%) and control cells (7 ± 1%) was not significantly different from each other. Had the subpopulation with high

Herceptin binding capacity been sensitive to the antibody treatment, its representation would have been less in the Herceptin-treated sample. Thus, we conclude that both subpopulations of JIMT-1 are Herceptin resistant.

Discussion

A cell line, JIMT-1, has been established from the pleural effusion of a Herceptin-resistant breast cancer patient. JIMT-1 retains *erbB2* oncogene amplification and its Herceptin-resistant phenotype *in vitro*.[5] In a search for the mechanism behind the Herceptin resistance of this cell line, we characterized its erbB expression profile and the expression of IGF-1R implicated in Herceptin resistance. We found no biologically significant alteration in the absolute numbers of proteins expressed, and thus their relative ratios, compared with three Herceptin-sensitive breast cancer cell lines. We concluded that differences in the erbB and IGF-1R expression levels could not account for the Herceptin resistance of JIMT-1 cells.

Binding of Herceptin to erbB2 is essential for its therapeutic action. We observed a diminished binding of Herceptin Mab to intact, nonpermeabilized JIMT-1 cells; the number of Herceptin binding sites was ~1/5 the number of erbB2 proteins expressed. This discrepancy was not the result of intracellular retention of erbB2, because another anti-erbB2 antibody, 2C4, was able to bind to erbB2 much more efficiently. The preservation of the binding efficiency of 2C4, which recognizes a membrane-distant epitope in the extracellular part of erbB2, suggested that the more membrane-proximal Herceptin epitope may have been masked. The binding capacity of Herceptin Fab was significantly higher than that of the whole antibody, confirming the hypothesis that a molecular block selectively hindered access of the larger IgGs to the Herceptin epitope. Detergent pretreatment increased the number of Herceptin Mab binding sites in JIMT-1, presumably by loosening the molecular associations preventing Herceptin binding. We gathered several additional lines of evidence supporting the hypothesis that the Herceptin epitope in JIMT-1 was masked: (a) APMA-induced a significantly higher level of increase in Herceptin-binding to JIMT-1 than in Herceptin-sensitive lines. (b) APMA treatment also increased the 2C4-binding capacity of JIMT-1 cells, but to a much smaller extent than that of Herceptin. This finding paralleled the higher level of 2C4 binding compared with Herceptin in untreated JIMT-1. We assume that in addition to erbB2, APMA-induced metalloproteases cleave other cell surface proteins, probably including MUC4, thereby decreasing the masking of epitopes on erbB2. The balance between APMA-induced cleavage and unmasking of erbB2 determines whether the binding of an antibody will increase or decrease upon APMA treatment. (c) We identified two subpopulations in JIMT-1 showing different Herceptin binding whereas expressing equal levels of erbB2. The low Herceptin-binding subpopulation expressed a higher level of MUC4, the molecule we propose to be responsible for masking the Herceptin epitope.

Rat Muc4 blocks the binding of anti-erbB2 antibodies, including Herceptin (37). We showed that MUC4 was expressed at a higher level in JIMT-1 compared with Herceptin-sensitive lines. Additionally, pixel-by-pixel analysis of MUC4 density and Herceptin fluorescence intensity revealed an inverse correlation between the two quantities. RNAi-mediated knockdown of MUC4 expression significantly increased the binding of Herceptin to the transfected subpopulation. Taken together, these results present strong evidence that MUC4 expression was the cause of the diminished binding of Herceptin to JIMT-1. It has been shown that overexpression of rat Muc4 induces tyrosine phosphorylation of erbB2 through a specific interaction between erbB2 and one of the EGF-like domains in the membrane-bound subunit of MUC4 (44). However, phosphorylation of erbB2 was weak in JIMT-1, although human MUC4 also contains EGF-like domains (40). One possibility is that the level of MUC4 expression was not high enough to cause erbB2 activation. The size of human MUC4 (4,500-8,500 amino acids; ref. 40) is significantly larger than that of the rat protein (3,000 amino acids; ref. 49). Thus, it is possible that the EGF-like domains in human MUC4 cannot orient properly and consequently cannot bind to erbB2 due to the

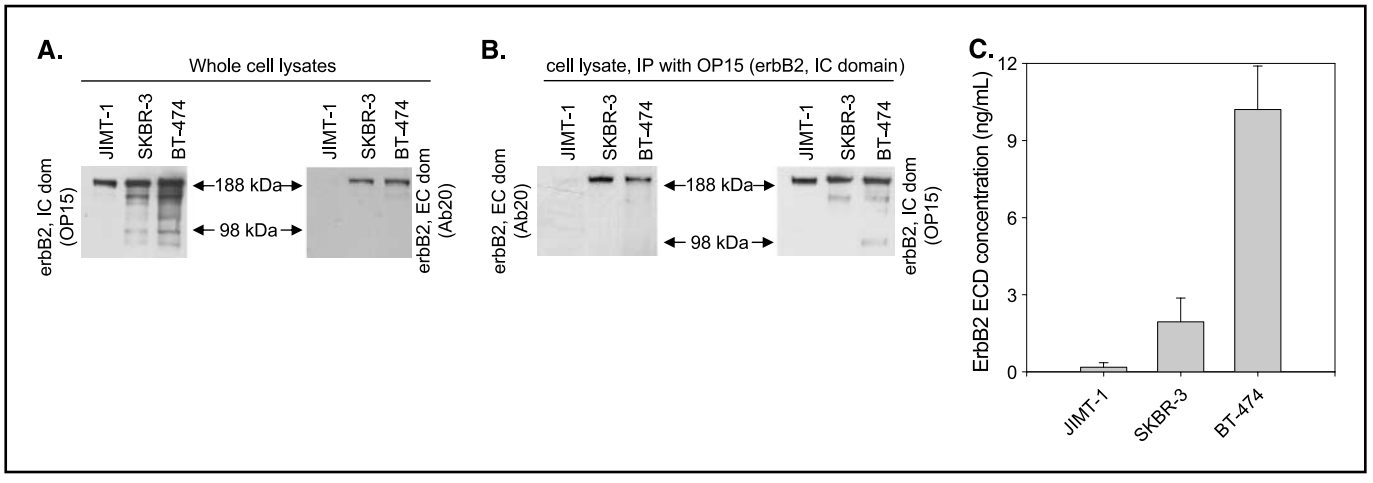

Figure 5. ErbB2 underwent less limited proteolysis in JIMT-1 cells and was recognized less efficiently by Ab20 than in Herceptin-sensitive lines. *A,* whole cell lysates probed with OP15, an antibody against an intracellular epitope on erbB2, then stripped and reprobed with Ab20, a cocktail of two antibodies against the extracellular region of erbB2. *B,* ErbB2 immunoprecipitated with OP15, separated by SDS-PAGE, and transferred to nitrocellulose. Membranes were first blotted with Ab20, then stripped and reprobed with OP15. *C,* Detection of the shed extracellular domain (*ECD*) of erbB2 in conditioned media. Cells were seeded at 80% confluency and conditioned media were assayed for the shed ECD of erbB2 using an ELISA kit. *Bars,* SE.

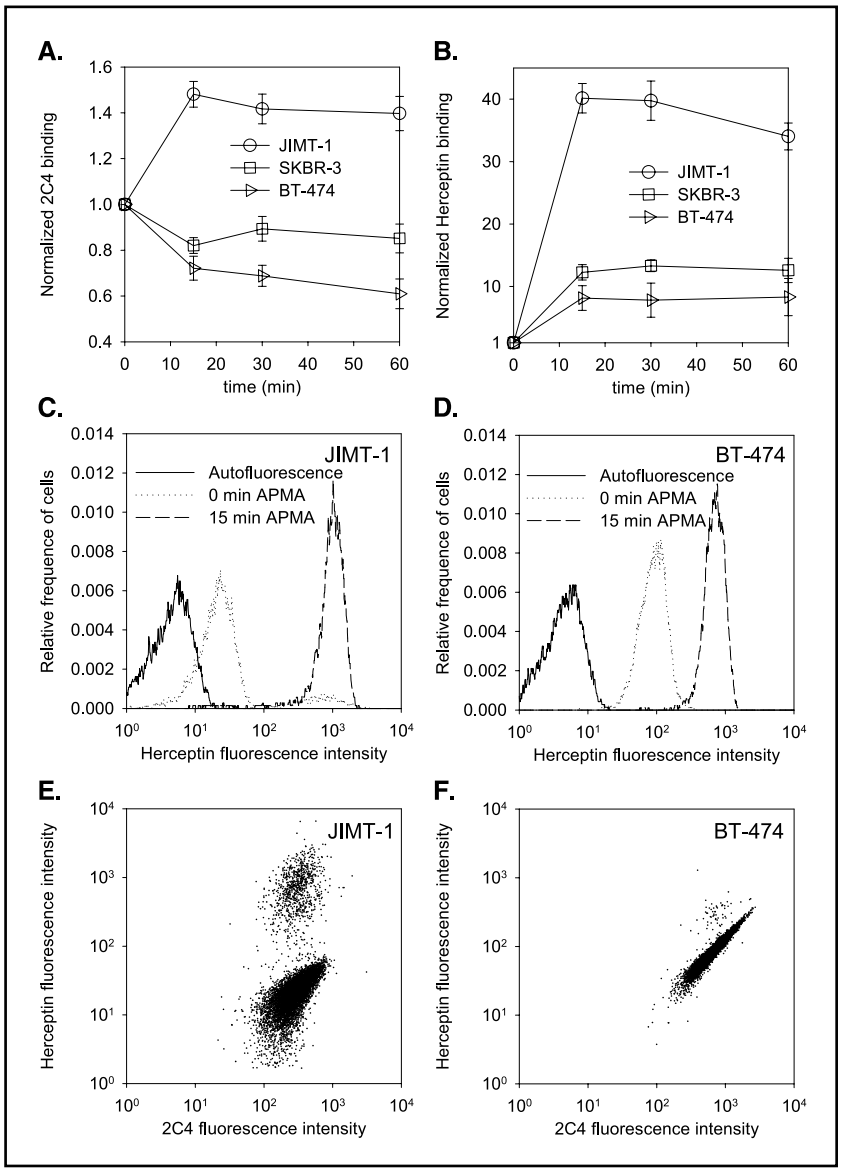

Figure 6. APMA-induced cleavage and unmasking of erbB2. *A* and *B*, normalized 2C4 or Herceptin binding to APMA-treated cells. Cells were treated with 1 mmol/L APMA followed by trypsinization and labeling with fluorescently tagged Mab 2C4 (*A*) or Herceptin (*B*). Mean fluorescence intensities determined by flow cytometry were normalized by the untreated intensity of the respective cell line. *Bars,* SE. *C* and *D*, flow cytometric histograms of JIMT-1 cells (*C*) and BT-474 cells (*D*) treated with APMA followed by labeling with fluorescent Herceptin. Histograms of untreated cells and cells treated with 1 mmol/L APMA for 0 and 15 minutes. The fluorescence histograms of SKBR-3 cells were very similar to those of BT-474 cells and are not shown. *E* and *F*, flow cytometric dot plots of untreated JIMT-1 (*E*) and BT-474 (*F*) cells double-labeled with Alexa488-conjugated 2C4 and Alexa633-conjugated Herceptin showing the correlation of Herceptin and 2C4 binding. The dot plot of SKBR-3 cells was very similar to that of BT-474 cells and is not presented.

presence of the bulky MUC4α domain. On the other hand, even if MUC4β can activate the kinase domain of erbB2, MUC4α may sterically hinder dimerization and cross-phosphorylation of erbB2. Other cell type–specific factors, including increased tyrosine phosphatase activity, may also inhibit or decrease activation of erbB2.

Herceptin-induced erbB2 internalization and down-regulation are thought to be causally related to the mechanism of action of the antibody, although formal proof for this hypothesis is lacking. We found that erbB2 is internalized and down-regulated by Herceptin treatment in JIMT-1 to an extent similar to that observed in Herceptin-sensitive lines. It is noteworthy that in the case of a cell line expressing 5 to 10×10^5 erbB2 per cell, a 20% to 40% down-regulation, the range usually observed, still leaves 3 to 8×10^5 erbB2 proteins on the cell surface, a number substantially higher than the normal expression level. Although it cannot be ruled out that even a relatively small decrease in erbB2 expression can have profound effects on a cell line that is "addicted" to overexpressed level of an oncogene (50), it is plausible that other actions of Herceptin also contribute to its therapeutic efficiency. The very low level of erbB2 activation in cultured JIMT-1 implies that erbB2 is not used and is therefore not required for the proliferation of JIMT-1. Thus, Herceptin-induced erbB2 down-regulation did not result in a decreased activation state of key signal transducing pathways. This circumstance explains the Herceptin-resistant phenotype of both the low and high Herceptin binding subpopulations of JIMT-1. We believe that the lack of erbB2 activation in JIMT-1 is the result of "molecular isolation" (i.e., a deprivation of erbB2 of its normal interaction and activation partners by MUC4). Previous studies have shown that rat Muc4 can localize erbB2 to the apical surfaces of polarized epithelial cells (51) thus sequestering it from other receptors and ligands present at the basolateral surface. Whether MUC4 can also sequester erbB2 in nonpolarized cells remains to be investigated. The low level of proteolytic processing of erbB2 is probably also caused by blocking access of metalloproteases to

erbB2 by MUC4. Thus, the constitutively active $p95^{erbB2}$ fragment (14) is absent in JIMT-1 and therefore cannot account for Herceptin resistance.

We propose the following model for the evolution of JIMT-1 cells. ErbB2 became overexpressed at an early stage of cancer progression and provided a survival/proliferation advantage. Later MUC4 became overexpressed, increasing the metastatic potential of the cells and protecting them from the immune system. Because MUC4 prevented association of erbB2 with its normal interaction partners, JIMT-1 cells required an alternative pathway leading to the activation of the mitogen-activated protein kinase and PI3K pathways. In this sense, overexpressed erbB2 is a "molecular fossil" reflected in its lack of activation. An important inference is that mere detection of erbB2 overexpression or amplification does not suffice for concluding that a cell line or patient is Herceptin responsive calling for functional assays in the selection of patients for Herceptin treatment. Indeed, it has been observed that patients with erbB2-phosphorylated breast cancer benefit more from Herceptin therapy than those without activated erbB2 (52). Diagnostic and treatment approaches based on a molecular understanding of the activation pathways of receptor tyrosine kinases will eventually lead to a more efficient and patient-specific treatment of malignant diseases.

Acknowledgments

Received 7/4/2004; revised 10/4/2004; accepted 11/11/2004.

Grant support: European Union grant FP5 QLRT-1999-3126 (ErbB in Breast Tumor), Max Planck Society, fellowship from the European Union grant (P. Nagy), and NIH grant CA74072 (development of 1G8).

The costs of publication of this article were defrayed in part by the payment of page charges. This article must therefore be hereby marked advertisement in accordance with 18 U.S.C. Section 1734 solely to indicate this fact.

References

1. Yarden Y, Sliwkowski MX. Untangling the ErbB signalling network. Nat Rev Mol Cell Biol 2001;2:127–37.
2. Tzahar E, Waterman H, Chen X, et al. A hierarchical network of interreceptor interactions determines signal transduction by Neu differentiation factor/neuregulin and epidermal growth factor. Mol Cell Biol 1996;16:5276–87.
3. Harris RC, Chung E, Coffey RJ. EGF receptor ligands. Exp Cell Res 2003;284:2–13.
4. Falls DL. Neuregulins: functions, forms, and signaling strategies. Exp Cell Res 2003;284:14–30.
5. Klapper LN, Glathe S, Vaisman N, et al. The ErbB-2/HER2 oncoprotein of human carcinomas may function solely as a shared coreceptor for multiple stroma-derived growth factors. Proc Natl Acad Sci U S A 1999;96:4995–5000.
6. Pinkas-Kramarski R, Lenferink AE, Bacus SS, et al. The oncogenic ErbB-2/ErbB-3 heterodimer is a surrogate receptor of the epidermal growth factor and betacellulin. Oncogene 1998;16:1249–58.
7. Karunagaran D, Tzahar E, Beerli RR, et al. ErbB-2 is a common auxiliary subunit of NDF and EGF receptors: implications for breast cancer. EMBO J 1996;15:254–64.
8. Holbro T, Beerli RR, Maurer F, Koziczak M, Barbas CF III, Hynes NE. The ErbB2/ErbB3 heterodimer functions as an oncogenic unit: ErbB2 requires ErbB3 to drive breast tumor cell proliferation. Proc Natl Acad Sci U S A 2003;100:8933–8.
9. Citri A, Skaria KB, Yarden Y. The deaf and the dumb: the biology of ErbB-2 and ErbB-3. Exp Cell Res 2003;284:54–65.
10. Lidke DS, Nagy P, Heintzmann R, et al. Quantum dot ligands provide new insights into erbB/HER receptor-mediated signal transduction. Nat Biotechnol 2004;22:198–203.
11. Wang Z, Zhang L, Yeung TK, Chen X. Endocytosis deficiency of epidermal growth factor (EGF) receptor-ErbB2 heterodimers in response to EGF stimulation. Mol Biol Cell 1999;10:1621–36.
12. Lenferink AE, Pinkas-Kramarski R, van de Poll ML, et al. Differential endocytic routing of homo- and hetero-dimeric ErbB tyrosine kinases confers signaling superiority to receptor heterodimers. EMBO J 1998;17:3385–97.
13. Worthylake R, Opresko LK, Wiley HS. ErbB-2 amplification inhibits down-regulation and induces constitutive activation of both erbB-2 and epidermal growth factor receptors. J Biol Chem 1999;274:8865–74.
14. Di Fiore PP, Pierce JH, Kraus MH, Segatto O, King CR, Aaronson SA. erbB-2 is a potent oncogene when overexpressed in NIH/3T3 cells. Science 1987;237:178–82.
15. Lonardo F, Di Marco E, King CR, et al. The normal erbB-2 product is an atypical receptor-like tyrosine kinase with constitutive activity in the absence of ligand. New Biol 1990;2:992–1003.
16. Revillion F, Bonneterre J, Peyrat JP. ERBB2 oncogene in human breast cancer and its clinical significance. Eur J Cancer 1998;34:791–808.
17. Shawver LK, Slamon D, Ullrich A. Smart drugs: tyrosine kinase inhibitors in cancer therapy. Cancer Cell 2002;1:117–23.
18. Slamon DJ, Leyland-Jones B, Shak S, et al. Use of chemotherapy plus a monoclonal antibody against HER2 for metastatic breast cancer that overexpresses HER2. N Engl J Med 2001;344:783–92.
19. Baselga J, Tripathy D, Mendelsohn J, et al. Phase II study of weekly intravenous recombinant humanized anti-p185HER2 monoclonal antibody in patients with HER2/*neu*-overexpressing metastatic breast cancer. J Clin Oncol 1996;14:737–44.
20. Agus DB, Akita RW, Fox WD, et al. Targeting ligand-activated ErbB2 signaling inhibits breast and prostate tumor growth. Cancer Cell 2002;2:127–37.
21. Allen LF, Eiseman IA, Fry DW, Lenehan PF. CI-1033, an irreversible pan-erbB receptor inhibitor and its potential application for the treatment of breast cancer. Semin Oncol 2003;30:65–78.
22. Nagy P, Bene L, Balázs M, et al. EGF-induced redistribution of erbB2 on breast tumor cells: Flow and image cytometric energy transfer measurements. Cytometry 1998;32:120–31.
23. Cho HS, Mason K, Ramyar KX, et al. Structure of the extracellular region of HER2 alone and in complex with the Herceptin Fab. Nature 2003;421:756–60.
24. Sarup JC, Johnson RM, King KL, et al. Characterization of an anti-p185HER2 monoclonal antibody that stimulates receptor function and inhibits tumor cell growth. Growth Regul 1991;1:72–82.
25. Nagy P, Vereb G, Sebestyen Z, et al. Lipid rafts and the local density of ErbB proteins influence the biological role of homo- and heteroassociations of ErbB2. J Cell Sci 2002;115:4251–62.
26. Neve RM, Nielsen UB, Kirpotin D, Poul MA, Marks JD, Benz CC. Biological effects of anti-ErbB2 single chain antibodies selected for internalizing function. Biochem Biophys Res Commun 2001;280:274–9.
27. Molina MA, Codony-Servat J, Albanell J, Rojo F, Arribas J, Baselga J. Trastuzumab (Herceptin), a humanized anti-Her2 receptor monoclonal antibody, inhibits basal and activated Her2 ectodomain cleavage in breast cancer cells. Cancer Res 2001;61:4744–9.
28. Yakes FM, Chinratanalab W, Ritter CA, King W, Seelig S, Arteaga CL. Herceptin-induced inhibition of phosphatidylinositol-3 kinase and Akt is required for antibody-mediated effects on p27, cyclin D1, and antitumor action. Cancer Res 2002;62:4132–41.
29. Sliwkowski MX, Lofgren JA, Lewis GD, Hotaling TE, Fendly BM, Fox JA. Nonclinical studies addressing the mechanism of action of trastuzumab (Herceptin). Semin Oncol 1999;26:60–70.
30. Kauraniemi P, Hautaniemi S, Autio R, et al. Effects of Herceptin treatment on global gene expression patterns in HER2-amplified and nonamplified breast cancer cell lines. Oncogene 2004;23:1010–3.
31. Clynes RA, Towers TL, Presta LG, Ravetch JV. Inhibitory Fc receptors modulate *in vivo* cytoxicity against tumor targets. Nat Med 2000;6:443–6.
32. Vogel CL, Cobleigh MA, Tripathy D, et al. Efficacy and safety of trastuzumab as a single agent in first-line treatment of HER2-overexpressing metastatic breast cancer. J Clin Oncol 2002;20:719–26.
33. Burris H III, Yardley D, Jones S, et al. Phase II trial of trastuzumab followed by weekly paclitaxel/carboplatin as first-line treatment for patients with metastatic breast cancer. J Clin Oncol 2004;22:1621–9.
34. Motoyama AB, Hynes NE, Lane HA. The efficacy of ErbB receptor-targeted anticancer therapeutics is influenced by the availability of epidermal growth factor-related peptides. Cancer Res 2002;62:3151–8.
35. Lu Y, Zi X, Zhao Y, Mascarenhas D, Pollak M. Insulin-like growth factor-I receptor signaling and resistance to trastuzumab (Herceptin). J Natl Cancer Inst 2001;93:1852–7.
36. Scott GK, Robles R, Park JW, et al. A truncated intracellular HER2/*neu* receptor produced by alternative RNA processing affects growth of human carcinoma cells. Mol Cell Biol 1993;13:2247–57.
37. Price-Schiavi SA, Jepson S, Li P, et al. Rat Muc4 (sialomucin complex) reduces binding of anti-ErbB2 antibodies to tumor cell surfaces, a potential mechanism for Herceptin resistance. Int J Cancer 2002;99:783–91.
38. Carraway KL, Price-Schiavi SA, Komatsu M, Jepson S, Perez A, Carraway CA. Muc4/sialomucin complex in the mammary gland and breast cancer. J Mammary Gland Biol Neoplasia 2001;6:323–37.
39. Escande F, Lemaitre L, Moniaux N, Batra SK, Aubert JP, Buisine MP. Genomic organization of MUC4 mucin gene. Towards the characterization of splice variants. Eur J Biochem 2002;269:3637–44.
40. Moniaux N, Nollet S, Porchet N, Degand P, Laine A, Aubert JP. Complete sequence of the human mucin MUC4: a putative cell membrane-associated mucin. Biochem J 1999;338:325–33.
41. Komatsu M, Yee L, Carraway KL. Overexpression of sialomucin complex, a rat homologue of MUC4, inhibits tumor killing by lymphokine-activated killer cells. Cancer Res 1999;59:2229–36.
42. Komatsu M, Tatum L, Altman NH, Carothers Carraway CA, Carraway KL. Potentiation of metastasis by cell surface sialomucin complex (rat MUC4), a

multifunctional anti-adhesive glycoprotein. Int J Cancer 2000;87:480–6.
43. Singh AP, Moniaux N, Chauhan SC, Meza JL, Batra SK. Inhibition of MUC4 expression suppresses pancreatic tumor cell growth and metastasis. Cancer Res 2004;64:622–30.
44. Carraway KL III, Rossi EA, Komatsu M, et al. An intramembrane modulator of the ErbB2 receptor tyrosine kinase that potentiates neuregulin signaling. J Biol Chem 1999;274:5263–6.
45. Jepson S, Komatsu M, Haq B, et al. Muc4/sialomucin complex, the intramembrane ErbB2 ligand, induces specific phosphorylation of ErbB2 and enhances expression of p27(kip), but does not activate mitogen-activated kinase or protein kinaseB/Akt pathways. Oncogene 2002;21:7524–32.
46. Zhang J, Perez A, Yasin M, et al. A new monoclonal antibody against MUC4 demonstrates the presence of MUC4 in human milk and at the luminal surfaces of blood vessels. J Cell Physiol. In press 2005.
47. Nagy P, Arndt-Jovin DJ, Jovin TM. Small interfering RNAs suppress the expression of endogenous and GFP-fused epidermal growth factor receptor (erbB1) and induce apoptosis in erbB1-overexpressing cells. Exp Cell Res 2003;285:39–49.
48. Elbashir SM, Harborth J, Lendeckel W, Yalcin A, Weber K, Tuschl T. Duplexes of 21-nucleotide RNAs mediate RNA interference in cultured mammalian cells. Nature 2001;411:494–8.
49. Sheng Z, Wu K, Carraway KL, Fregien N. Molecular cloning of the transmembrane component of the 13762 mammary adenocarcinoma sialomucin complex. A new member of the epidermal growth factor superfamily. J Biol Chem 1992;267:16341–6.
50. Weinstein IB. Addiction to oncogenes: the Achilles heel of cancer. Science 2002;297:63–4.
51. Ramsauer VP, Carraway CA, Salas PJ, Carraway KL. Muc4/sialomucin complex, the intramembrane ErbB2 ligand, translocates ErbB2 to the apical surface in polarized epithelial cells. J Biol Chem 2003;278:30142–7.
52. Hudelist G, Kostler WJ, Attems J, et al. Her-2/*neu*-triggered intracellular tyrosine kinase activation: *in vivo* relevance of ligand-independent activation mechanisms and impact upon the efficacy of trastuzumab-based treatment. Br J Cancer 2003;89:983–91.